

# Spatial Structure of Low-Frequency Hall-MHD Wave Propagation in a Field-Reversed Configuration Plasma

Takuya TAKAHASHI<sup>1)</sup>, Toru TAKAHASHI<sup>1)</sup>, Toshiki TAKAHASHI<sup>1)\*</sup>,  
Siyu ZHANG<sup>1)</sup>, Shun INOUE<sup>1)</sup>, Tomohiko ASAI<sup>2)</sup>, Naoki MIZUGUCHI<sup>3)</sup>

<sup>1)</sup> Graduate School of Science and Technology, Gunma University, 1-5-1 Tenjin-cho, Kiryu, Gunma 376-8515, Japan

<sup>2)</sup> College of Science and Technology, Nihon University, Tokyo 101-8308, Japan

<sup>3)</sup> National Institute for Fusion Science, National Institutes of Natural Sciences, 322-6 Oroshi-cho, Toki, Gifu 509-5292, Japan

(Received 27 June 2025 / Accepted 3 July 2025)

A linear Hall-MHD simulation code is developed to investigate the spatial structure of two-dimensional wave propagation excited in a field-reversed configuration (FRC) equilibrium plasma. A low-frequency oscillating magnetic field at 160 kHz is externally applied by a ring coil installed concentrically with the device axis in the open-field region. The generated toroidal magnetic field propagates primarily along magnetic field lines at a phase velocity comparable to that of shear Alfvén waves. Due to the Hall effect, toroidal magnetic fluctuations penetrate into the closed-field region near the separatrix over a distance on the order of the ion skin depth. In the core region, where magnetic fluctuations vanish, ion density oscillations become dominant.

© 2025 The Japan Society of Plasma Science and Nuclear Fusion Research

Keywords: Hall-MHD, low-frequency wave, field-reversed configuration, numerical simulation

DOI: 10.1585/pfr.20.1203042

Heating of field-reversed configuration (FRC) plasmas in the regime of extremely high beta is inherently challenging due to the strong magnetic non-uniformity, which severely localizes the cyclotron resonance regions. Nevertheless, FRCs possess a unique magnetic topology well-suited for confining high-energy ions with large angular momentum and Larmor radii comparable to the system size [1]. As a result, neutral beam injection (NBI) remains the primary method for heating and sustaining FRC plasmas [2, 3].

However, in view of developing FRCs as core plasmas for fusion reactors, it is imperative to explore alternative heating schemes that could enhance operational flexibility and reactor design freedom. In this context, past experiments on the FIX device at Osaka University demonstrated wave excitation using ring coils positioned in the open-field-line region, where wave propagation with phase velocities comparable to those of shear Alfvén waves was observed [4]. Complementary particle-in-cell (PIC) simulations reproduced these observations and revealed a cutoff of electromagnetic fluctuations near the separatrix, along with density fluctuations associated with the compression and expansion of the separatrix layer [5].

In this study, we have developed a new Hall-MHD linear wave analysis code to investigate the spatial structure of wave propagation in FRCs, where the closed magnetic field line region is surrounded by an open-field-line region and can sustain plasma pressure comparable to the external magnetic

pressure. By comparing our results with those of PIC simulations, we aim to elucidate the role of kinetic effects in wave dynamics within FRC plasmas. This paper reports the results of a two-dimensional low-frequency Hall-MHD linear wave analysis in FRC geometry using the newly developed code.

Wave propagation was analyzed using the linearized Hall-MHD equations. To validate the numerical code, a benchmark test was conducted by comparing the simulation results with an analytically tractable wave solution characterized by a density perturbation of the form  $n_1 = \epsilon n_0 J_0(kr) \cos(kz - \omega t)$ , propagating along the axis of a cylinder in a uniform magnetic field. Here,  $\epsilon = 10^{-3}$  is a small perturbation parameter,  $J_0(kr)$  is the zeroth-order Bessel function of the first kind,  $n_0$  is the unperturbed uniform density,  $k$  is the wavenumber,  $\omega$  is the angular frequency,  $T$  is the total plasma temperature defined as the sum of ion and electron temperatures, and  $m$  is the proton mass. The theoretical phase velocity of this wave is given by  $\omega/k = \sqrt{2T/m}$ . The simulation reproduced this phase velocity with less than 1% error, thereby confirming the validity of the code. Further details of the benchmark analysis will be presented in a separate publication.

In this study, the analysis domain was based on the confinement region of the FAT-CM device at Nihon University [6]. The geometry and computational parameters used are summarized in Table 1. The equilibrium magnetic field configuration was obtained by solving the Grad-Shafranov equation, and the equilibrium flow velocity was assumed to be  $\mathbf{u}_0 = \mathbf{0}$ . To maintain consistency with this assumption, the equilibrium electric field was specified as  $\mathbf{E}_0 = (T_i/en_0)\nabla n_0$ .

\*Corresponding author's e-mail: t-tak@gunma-u.ac.jp

Table 1. Parameters of the confinement vessel and plasma.

|                                      |       |      |
|--------------------------------------|-------|------|
| Confinement vessel radius $r_w$      | 3.875 | [m]  |
| Confinement vessel half length $z_m$ | 1.12  | [m]  |
| Ion temperature $T_i$                | 66.0  | [eV] |
| Electron temperature $T_e$           | 34.0  | [eV] |
| Plasma temperature $T = T_i + T_e$   | 100.0 | [eV] |

Figure 1 shows the two-dimensional  $r$ - $z$  distribution of the toroidal magnetic field  $B_{\theta 1}$  excited by a ring current with an antenna frequency of  $f_{\text{ANT}} = 112$  kHz. The three panels correspond to (a)  $t = 0.0440$   $\mu\text{s}$ , (b)  $t = 7.26$   $\mu\text{s}$ , and (c)  $t = 14.5$   $\mu\text{s}$ , from top to bottom. The position of the ring current and the shape of the separatrix are depicted in Fig. 1(a). The ring current excites a toroidal magnetic field  $B_{\theta 1}$ , which is typically absent in the field-reversed configuration (FRC) plasma. The excited magnetic field wave predominantly propagates along the magnetic field lines and travels at a nearly constant speed outside the FRC plasma. Inside the FRC, the wave amplitude becomes significantly smaller than in the surrounding regions.

To elucidate the spatial distribution of magnetic field fluctuations, the radial profiles of the toroidal magnetic field  $B_{\theta 1}$  at the midplane ( $z = 0$ ) are presented in Fig. 2. The plots correspond to four equally spaced time slices:  $t = 11.0$ , 11.9, 12.8, and 13.7  $\mu\text{s}$ , arranged from top to bottom at 0.9  $\mu\text{s}$  intervals. The position of the separatrix is indicated by a vertical dashed-dotted line.

The results indicate that the  $B_{\theta 1}$  wave is not completely reflected or blocked at the separatrix, but partially penetrates into the FRC plasma and undergoes strong attenuation. The estimated penetration depth into the separatrix region is approximately 0.019–0.039 m.

This penetration is considered to result from the Hall term. Under the conditions of this study, the strength of the two-fluid effects evaluated at the maximum plasma density is characterized by the parameter  $S_* \equiv (r_s \omega_{pi})/c = 0.56$ , where  $\omega_{pi}$  is the ion plasma frequency, and  $c$  is the speed of light. The corresponding ion penetration length is given by  $\ell_i = r_s/S_* = 0.0243$  m. Although this value is slightly shorter than the penetration length obtained from numerical calculations, the agreement is reasonable considering that  $S_*$  is defined using the peak plasma density. Under the present simulation condition, where the magnetic field strength at the separatrix is 0.012 T, the ion gyroradius is approximately 0.1 m; this is about three times larger than the observed  $\ell_i$ . Nevertheless, the spatial structure of the fluctuating fields obtained using a hybrid model that incorporates ion kinetics [5] remains essentially consistent with the present results. This indicates that kinetic effects on wave propagation near the separatrix are minor.

Figure 3 shows the radial distribution of the wave propagation velocity at the midplane ( $z = 0$ ) for waves excited by the ring current. Inside the FRC plasma, where the magnetic field perturbation  $B_{\theta 1}$  does not propagate, the propagation velocity was inferred from the ion density fluctuation  $n_1$  as

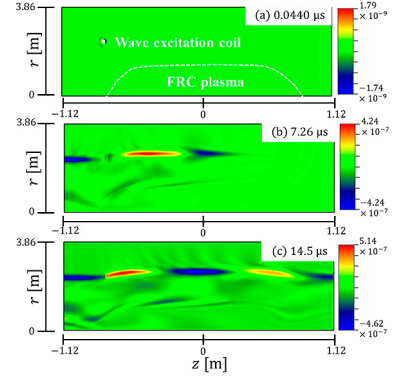


Fig. 1. Two-dimensional  $r$ - $z$  distribution of the toroidal magnetic field  $B_{\theta 1}$  excited by the ring current. From top to bottom: (a)  $t = 0.0440$   $\mu\text{s}$ , (b)  $t = 7.26$   $\mu\text{s}$ , and (c)  $t = 14.5$   $\mu\text{s}$ . The positions of the ring antenna and the separatrix are indicated in (a).

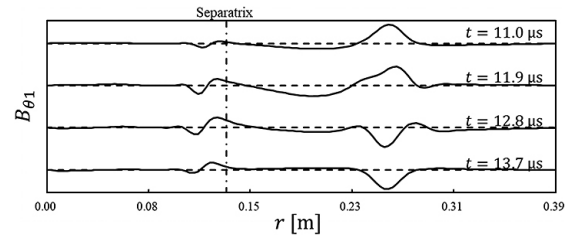


Fig. 2. Radial profiles of the toroidal magnetic field perturbation  $B_{\theta 1}$  at the midplane ( $z = 0$ ). Profiles at  $t = 11.0$ , 11.9, 12.8, and 13.7  $\mu\text{s}$  are plotted sequentially from top to bottom at equal vertical intervals. The vertical dashed-dotted line indicates the position of the separatrix.

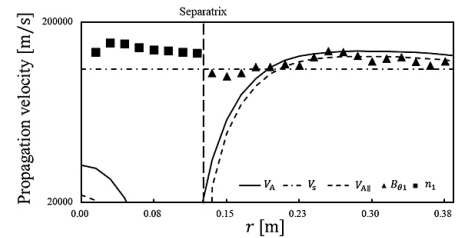


Fig. 3. Radial profile of the propagation velocity at the midplane ( $z = 0$ ). The solid line represents the Alfvén velocity ( $V_A$ ), the dash-dotted line indicates the ion acoustic speed ( $V_s$ ), and the dashed line shows the shear Alfvén velocity ( $V_{A||}$ ) based on theoretical estimates. The simulation results for the propagation velocity derived from the toroidal magnetic field and the density fluctuations are indicated by  $\blacktriangle$  and  $\blacksquare$ , respectively.

a substitute.

Outside the separatrix ( $r \geq r_s$ ), the waves propagated at approximately the shear Alfvén velocity  $V_{A||}$  in regions where  $V_{A||} > V_s$  (the ion acoustic speed), and at approximately the ion acoustic speed  $V_s$  where  $V_{A||} \leq V_s$ . Inside the separatrix ( $r \leq r_s$ ), the propagation velocity was found to be comparable to the shear Alfvén velocity  $V_{A||}$  near the confinement vessel wall.

This work was performed with the support and under the auspices of the NIFS Collaboration Research program (NIFS22KIPT006 and NIFS22KIST016).

- [1] J.M. Finn and R.N. Sudan, Nucl. Fusion **22**, 1443 (1982).
- [2] T. Asai *et al.*, Phys. Plasmas **7**, 2294 (2000).
- [3] H. Gota *et al.*, Nucl. Fusion **61**, 106039 (2021).
- [4] S. Okada *et al.*, Nucl. Fusion **47**, 677 (2007).
- [5] T. Urano *et al.*, Nucl. Fusion **62**, 026019 (2022).
- [6] T. Asai *et al.*, Nucl. Fusion **61**, 096032 (2021).